Environ Ecol Stat (2009) 16:133–151
DOI 10.1007/s10651-007-0079-z

A stochastic forest fire growth model

Den Boychuk · W. John Braun · Reg J. Kulperger · Zinovi L. Krougly · David A. Stanford

Received: 1 March 2006 / Revised: 1 July 2006 / Published online: 8 March 2008

Abstract We consider a stochastic fire growth model, with the aim of predicting the behaviour of large forest fires. Such a model can describe not only average growth, but also the variability of the growth. Implementing such a model in a computing environment allows one to obtain probability contour plots, burn size distributions, and distributions of time to specified events. Such a model also allows the incorporation of a stochastic spotting mechanism.

Keywords Stochastic fire spread · Markov model · Lattice · Spatial model · Rate of spread

1 Introduction

Prediction of forest fire behaviour is an important element in the management of forests, as well as in assessing ecological effects. Conceptually, fire prediction models fall into two categories: deterministic and stochastic. Most fire prediction models are deterministic, incorporating physical mechanisms for fire spread. An early influential model of this type is the "Rothermel model" (Rothermel 1972). FARSITE (Finney 1999) is the most popular of the deterministic and mechanistic models of forest fire growth and spread. Another important deterministic model is Prometheus (2006). See also Berjak and Hearne (2002) for an example of a deterministic lattice model and for references to earlier deterministic models.

D. Boychuk
Ontario Ministry of Natural Resources, Sault Ste Marie, Ontario, Canada

W. J. Braun · R. J. Kulperger (✉) · Z. L. Krougly · D. A. Stanford
Department of Statistical and Actuarial Sciences, University of Western Ontario, London, Ontario, Canada N6A5B9
e-mail: kulperger@stats.uwo.ca

None of these models allow for stochastic variability of the output, other than by varying the initial conditions or varying the weather or fuel type. Once those conditions are set, the output is deterministic, so that running the model twice yields the same output both times. While this may produce quite realistic average patterns, it does not produce stochastic output such as probability contours of regions burned. There are variables which are not accounted for, and perhaps other random effects, which can have a subtle or large impact on the spread in any particular fire. One important such random phenomenon is fire spotting, in which an airborne burning firebrand is carried ahead of the fire line, leading to a fresh fire start. A stochastic model has the possibility of taking this into account.

The stochastic approach, which we pursue here, models a fire as a random phenomenon on a grid of spatial locations. Our model is an example of an interacting particle system; it is a continuous-time Markov chain on a lattice. Each lattice location represents a small region, for example a $156.25\,\mathrm{m}^2$ as used in Sect. 3.

Each lattice site changes state according to local transition rates. These rate functions model the competing physical processes of fire spread, spotting, and burnout. The rate functions are based on covariate information which can be obtained for each lattice site, such as topography, fuel moisture and local weather. The form of these functions is tentative; providing a satisfactory model for them is beyond the scope of the present paper.

While the rate functions proposed in this paper may not be in a physically reasonable form at this time, we will see that they can be calibrated to replicate phenomena such as the wildfire spread seen in the Dogrib case. For some information on the Dogrib fire see the Prometheus web site (Prometheus 2006). In particular, the proposed spotting mechanism allows the simulated fire to jump the small river, and continue spreading on the other side, providing a first hint of model validity. Questions of more general model validation are also beyond the scope of this paper.

Since stochastic patterns are generated by our model, probability contours of areas burned may be produced, either analytically, or more reasonably by simulation. In addition, the simulation models can easily yield empirical distributions of other phenomena such as total area burned by a fixed point in time, or empirical distributions of the time to reach or cross a barrier such as a river.

Our view is that the model presented here can complement rather than compete with the more popular deterministic models. As it develops, we hope it will become another tool in the arsenal of tools used by foresters.

Although we believe our proposed stochastic model will be a useful conceptual tool, it is not the first stochastic fire spread model to be proposed. Other stochastic models in the forest fire literature are in the class of percolation models (for example, Stauffer and Aharony 1992). These models have a fractal-like shape with unburnt holes due to the random initial placement of trees. Although the model we are proposing can be analyzed using percolation methods (see, for example, Durrett 1988), its dynamics are quite different from the percolation models that have been proposed for fire spread. Furthermore, it is well known that the boundary of the proposed model does not exhibit fractal behaviour. A very different stochastic model is the one studied by Malamud et al. (1998) which gives correct fire area power law behaviour, but cannot be used to predict actual fire dynamics.

Anderson et al. (2005) used ensemble modeling to generate probability contour maps of the perimeter from a deterministic fire growth model. This was done by perturbing input weather by random or systematic amounts over simulated time. This differs from our approach in that in ensemble modeling, the perturbations apply deterministically to the entire fire at each time step, while in our approach, the stochastic behaviour varies over space at each instant. Spatially-varying randomness is a suitable representation of local wind gusts and local fuel heterogeneity. Further, the deterministic fire growth model cannot generate stochastic fire spotting.

The only other stochastic fire spread model we are aware of is Ntaimo et al. (2004), but as that is not a Markov process, it is less amenable to extensions of time varying external covariates such as changing weather.

The remainder of the paper is organized as follows. Section 2 discusses the lattice model structure. Subsections of this discuss extensions to time varying rates, incorporating wind, both speed and direction, and a spotting mechanism. Section 3 discusses the Dogrib fire event, and one version of the model to describe that type of phenomenon. Section 4 gives some concluding remarks.

2 Overview of the lattice model

In this section, we overview the spread model in an attempt to demonstrate the basic mechanisms. We first describe the model without a spotting mechanism. For notational convenience, we suppose the external covariates are constant with respect to time. In the next subsection we will relax this assumption.

On the landscape where the simulated forest fire will grow, we overlay an m by n regular grid or lattice of locations.

A lattice point may be in one of several states, corresponding to a local state of a forest fire. These states are combustible fuel (F), burning fuel (B) and burnt out fuel (O), as well as a non-fuel state from which no transitions may take place (NF). The times to transit from F to B and from B to O are independent, and exponentially distributed, given the current configuration. The NF states represent non-combustible things such as water or rock.

Once a cell has reached state O, that cell can no longer leave that state. State O acts like an absorbing state. Thus we need not distinguish between the burnt out state O or any other cell with no fuel NF, so for the remainder of this section we confine our attention to this simpler set of possible states (F, B, O).

At a given time t, $x_{(i,j)}(t)$ is defined as the state of the lattice location at (i, j). It can take any one of the values F, B, O.

The transition rate from one state to another at a lattice point depends on what is happening in the neighbourhood of the lattice point. We consider a neighbourhood which consists of the given lattice point plus its four nearest neighbours, those points which are immediately to the north, south, east and west. The (i, j)th lattice location will then have a neighbourhood given by

$$\mathcal{N}(i, j) = \{(i, j), (i, j + 1), (i, j - 1), (i + 1, j), (i - 1, j)\}.$$

The set of states in the neighbourhood of (i, j) at time t is given by

$$X_{\mathcal{N}(i,j)}(t) = \{x_{(i,j)}(t) : (i, j) \in \mathcal{N}(i, j)\}. \tag{1}$$

If $x_{(i,j)}(t) = \mathsf{F}$, we may expect that $x_{(i,j)}(s) = \mathsf{B}$ for some time $s > t$. The rate at which this transition will occur depends on the states of the lattice points in its neighbourhood (i.e., the points in $\mathcal{N}(i, j)$). The rate function for this transition from state F to state B is given by

$$r_{(i,j)}(\mathsf{F}, \mathsf{B}; w, g) = f((i, j), X_{\mathcal{N}(i,j)}, w, g) \tag{2}$$

where w contains the weather and other external covariate information at (i, j), and g contains the information about the terrain at (i, j) and possibly at neighbouring lattice sites. The model assumptions that we make allow us to write

$$f((i, j), X_{\mathcal{N}}(i, j); w, g) = \sum_{(k,l)\in\mathcal{N}(i,j)} \lambda((i, j), (k, l), x_{(k,l)}, w, g) \tag{3}$$

where $\lambda((i, j), (k, l), x_{(k,l)}, w, g)$ is a function of individual neighbourhood state values, weather and geography. Typically $\lambda((i, j), (i, j), w, g)$ is constant, depending only on w and g, to reflect spontaneous fires due to lightning or human causes. Since the physical rules governing the system are the same wherever one is located, there is a spatial stationarity which allows us to express the rate functions in terms of the coordinate-wise difference between a site (i, j) and its neighbours (k, l). That is (4), where f_0 is a specified function

$$\lambda((i, j), (k, l), x_{(k,l)}, w, g) = f_0((k, l) - (i, j), x_{(k,l)}, w(k, l), g). \tag{4}$$

This means that the rate function is determined by a simple translation of the function f_0 to each location centred at (i, j). Thus we need only to specify the function $f_0((k, l))$ at location arguments (k, l) for each point in the neighbourhood $\mathcal{N}(0, 0)$.

Specifying the rate functions r allows one to incorporate various pieces of physical information, topography and other fire behaviour dynamics. The most important aspects of weather are wind speed and direction, temperature, and fuel moisture content. These may in turn be captured through moisture codes and fire receptivity indices, such as those used by the Forestry Canada Fire Danger Group (1992). (Two important indices are the fine-fuel moisture code (FFMC) for the top stratum of surface material, and duff moisture code for the next stratum. We employ the FFMC in our model.)

Similarly we have transitions from the burning state B to the burnt out state O governed by rate

$$r_{(i,j)}(\mathsf{B}, \mathsf{O}; w, g) = \lambda((i, j), x_{(i,j)}, w, g). \tag{5}$$

This rate depends only on its own site (not on the more general neighbourhood), and on the configuration at it own site, namely B, and so is of the same functional structure as above. In our model we take this to be a constant with respect to time and space,

depending only on the weather. It could be modified to include information about neighbouring sites.

All other transitions have rate functions that are null.

Writing the simulation code can and should be done to take advantage of some numerical and programming efficiencies, as there are different ways of implementing a Markov chain in code. This is discussed later.

We conclude this subsection with several observations. One could consider larger neighbourhood structures, such as incorporating eight nearest neighbours, at a cost of additional computational effort. In a limited numerical study of the most basic specific form of these models, a larger neighbourhood did not lead to qualitatively different output, so we retained the simpler neighbourhood form given by $\mathcal{N}(i, j)$. One could also consider a larger set of states, allowing for different fuel types or moisture levels for instance. Finally, there is the question of grid size. A finer grid requires more computing power to implement, and there is also the consideration of the degree of fine structure information available. One could also use a larger scale, but that might aggregate too large a local area, thus not taking into sufficient account local fire growth factors.

2.1 Time varying rates

The model can be extended to include time varying components. The main difference is that the Markov chain is no longer time homogeneous. This affects the computations substantially.

Notationally the changes require that (2) becomes

$$r_{(i,j)}(\mathsf{F}, \mathsf{B}; w, g, t) = f((i, j), X_{\mathcal{N}(i,j)}(t), w(t), g(t)) \tag{6}$$

and (5) becomes

$$r_{(i,j)}(\mathsf{B}, \mathsf{O}; w, g, t) = \lambda((i, j), x_{(i,j)}, w(t), g(t)). \tag{7}$$

The rate functions r now depend on $w(t)$, the weather at time t, and diurnal variation, of the temperature.

The simplest implementation to this time inhomogenous Markov chain is to approximate it as a sequence of time homogeneous Markov chains. In other words one can replace the rates as a function of time t with piecewise constant rates. Over the course of a day, time is divided into smaller segments, where on each segment weather will be treated as constant for that segment. From the beginning to the end of that segment, the Markov chain is time homogeneous. The end state of the system at one time segment will be the input state of the system for the next segment.

2.2 Incorporating wind

Fuel type and slope play an important role in the spread of fire (Canadian Forestry Service 1992). We assume a homogeneous fuel-type. Wind plays a crucial role in

forest fire spread. It is dynamic, changing on a much faster time scale. In moderate to high wind, an assumption of time inhomogenous Markov parameters is probably not reasonable, except on a very short time scale. Specifically the rates for the competing exponential times in (3) need to be replaced by functions of time.

There are two basic rate of spread (ROS) functions. They are $\lambda^b(t)$, the base rate of spread, a function of fuel type but with no wind and flat ground, and $\lambda^m(t)$, the maximum ROS, again a function of fuel type and maximum wind speed.

We now define the basic translation rate parameter function, the analogue of (4) where angles are in terms of compass coordinates. Let

$$\theta_{(k,l)} = \begin{cases} \pi & \text{if } (k,l) = (0,-1) \quad \text{(South)} \\ 0.5\pi & \text{if } (k,l) = (1,0) \quad \text{(East)} \\ 1.5\pi & \text{if } (k,l) = (-1,0) \quad \text{(West)} \\ 0 & \text{if } (k,l) = (0,1) \quad \text{(North).} \end{cases} \tag{8}$$

Adapting a formula of Xu and Lathrop (1994) we use as in Boychuck et al. (2007)

$$f_0((k,l), \mathsf{B}, w, g)(t) = \frac{c(t)\lambda^b(t)}{1 - \cos(\theta_{(k,l)} - \theta^m(t))[1 - \lambda^b(t)/\lambda^m(t)]} \tag{9}$$

as the rate of the exponentially distributed time until fire spreads from a burning site to its nearest-neighbour in direction $\theta^m(t)$. Since fire cannot spread from a non-burning cell

$$f_0((k,l), \mathsf{O}, w, g)(t) = 0$$
$$f_0((k,l), \mathsf{NF}, w, g)(t) = 0\,.$$

The function $c(t)$ can be further used to incorporate a diurnal cycle.

The rate functions constructed via (9) and (4) no longer are parameters of exponential distributions.

The time-evolving rates into the model introduced in Sect. 2.1 are nontrivial to implement. It is possible to adapt a thinning algorithm used for simulating non-homogeneous Poisson processes (Lewis and Shedler 1976), but we believe this will be more complicated to implement than the piecewise constant approach taken here.

2.3 Spotting mechanism

One area where stochastic simulators have a distinct advantage over deterministic ones pertains to the incorporation of important random events, such as the spotting of fresh fires. The fire spread model presented here includes a mechanism to simulate the spotting of new fires. Spot fires are difficult to model because the underlying physical process is difficult to observe and measure. The process is highly stochastic and involves the generation of embers from within intense fires, their loft in a smoky, turbulent convection column, their gradual consumption by fire often to the point of

extinction, their drift due to wind and gravity, and their possible landing on receptive fuels. Chase (1984) describes a commonly used model of spot fire distances. Our algorithm to incorporate fire spotting has the same general structure, but is simplified as described below.

1. The occurrence of a firebrand being sent aloft is treated as a competing Poisson event to the rates of spread to adjacent cells and of fire burnout in the existing cell. The various instantaneous rate functionals for each of these events can be quite general in nature, but we cannot go beyond the family of competing Poisson processes without sacrificing the memoryless property which enables us to process the next event without regard for other possible future events.
2. When a firebrand becomes airborne, its time aloft is determined. We presently assume an exponentially-distributed time aloft for simplicity.
3. The likelihood it is still burning or smoldering upon landing is determined. Currently, we assume that the time to burnout is exponentially distributed. Only if it has not burned out do we need to proceed to the next step.
4. The landing location of a burning or smoldering firebrand is found as a function of its time aloft and the predominant wind direction, subject to a random jitter that is bivariate-normally distributed.
5. In the final step, it is determined if the burning or smoldering firebrand has landed upon fuel, and if so, a final Bernoulli random, varriable is generated to determine if ignition occurs.

There are several generalizations that our algorithm can accommodate. As the time scale that a firebrand is aloft is so much smaller than the time scale for individual lattice points to change state, we can view the time aloft as essentially instantaneous. As such, there would be no impact on the "next event" characteristic if we were to allow for quite arbitrary distributions of time aloft, or for that matter, time alight. However, we observe that several general distributions for time aloft or alight could still be accommodated theoretically within our framework if the time scales were comparable, such as integer-shape-parameter Gamma distributions and phase-type distributions.

In a similar fashion, our algorithm can be readily generalized to allow the probability of successful ignition to decrease with time aloft, as well as local parameters such as fuel type. This would be most easily achieved via another exponential term, but again, an arbitrary monotonically-decreasing density would do.

We note that the vast majority of firebrands are never observed, due to failing one of the successive steps leading to a fresh ignition: (a) not transcending the boundaries of the existing fire in a perceptible fashion, (b) burning out prior to landing, (c) not landing on a fuel type, and (d) not spotting a new fire despite the capability of doing so. The end result is a highly censored process, which poses a number of statistical challenges when tuning the parameter values. The flexibility of our algorithm in accommodating a wide range of distribution types for these spotting phenomena will be very beneficial as more is learned about them, so that more accurate choices can be made where warranted.

The incorporation of the firebrand in terms of rate functions is incorporated by adding an additional rate

$$\sum_{(k,l)} \lambda_S((i,j),(k,j),x_{(k,l)},w,g) \tag{10}$$

where the sum is over all lattice points. This notation is to be consistent with (3). It is the rate at which a burning cell at site (k,l), and hence the value $x_{(k,l)} = \mathsf{B}$, transmits a firebrand to a cell at a location (i,j), which may be far away, not just in the neighbourhood $\mathcal{N}(i,j)$.

The rate (3) is now replaced by

$$r_{(i,j)}(\mathsf{F},\mathsf{B}) = \sum_{(k,l)\in\mathcal{N}(i,j)} \lambda((i,j),(k,l),x_{(k,l)},w,g) + \sum_{(k,l)} \lambda_S((i,j),x_{(k,l)},w,g). \tag{11}$$

The rate (10) could be implemented in a numerical code by a product of the terms given in the itemized list above describing the spotting mechanism. Specifically it would involve summing over only burning cells that can produce firebrands and potential spottings. The Eq. (11) sums the net spotting impact on destination cell (i,j) by summing over all source cells (k,l) that are capable of dispatching a firebrand to (i,j). Computationally, this is inefficient. So long as the frequency of spotting events is properly accounted for, we are free to record these either from the perspective of the issuing cell outwards, or the destination cell inwards, as both approaches will account for all instances of spotting once. The former view is computationally much faster as we need only consider the rate at which the source cell issues firebrands, and we need not concern ourselves with where they are actually landing. That facet has been subsumed in steps 1–5 of our spotting algorithm.

Our goal here has been to point out the capability of a stochastic simulator as a vehicle to readily incorporate the spotting of new fires. An example in the next section incorporates the fire spotting mechanism described above.

3 Simulation of the Dogrib large fire event

The example in this section is the result of an attempt to produce similar spread behaviour to that seen in the Dogrib fire which occurred near Nordegg, Alberta, starting on September 25th, 2001 and ending on October 21st (see Fig. 1). A detailed description and analysis of the fire is given in Trevis (2005).

On October 16, a "wind event" occurred: high winds blew in a northeasterly direction, and in the space of about 13 h the fire consumed almost 10 times as much area as it had over the course of the previous 21 days. Its size at 11:30 p.m. on October 16, 2001 comprised 9,898 ha. We attempt to reproduce, using simulations from our proposed model, the type of behaviour as seen in the Dogrib system during this October 16 episode.

Our replications of the October 16th event were achieved by conceptually "igniting" a fire in the southwest corner of the map, just north of the river at the bend. This was done to provide the closest basis for comparison with Prometheus runs "ignited" at a similar location (see, for example, Fig. 2). The region covered by the simulation

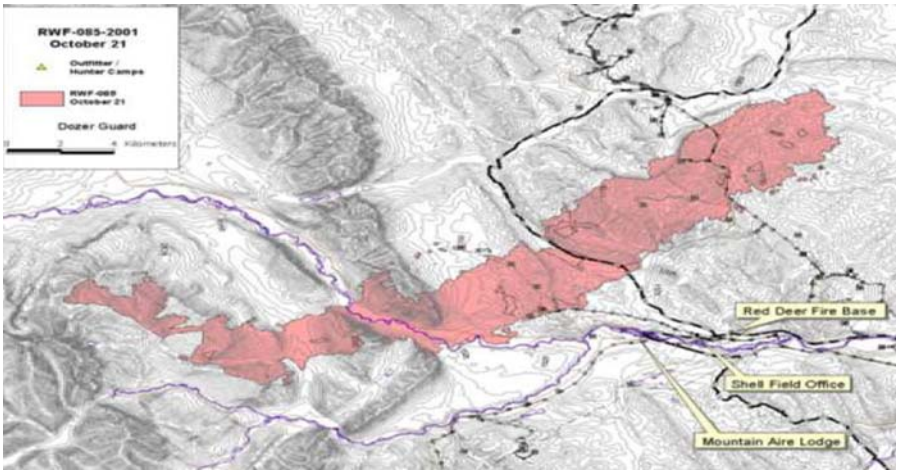

Fig. 1 Dogrib fire started on September 25, 2001 near Nordegg, in central Alberta

was a 5×5 km square (although the figures we present display a rectangular area not covering the full vertical range). This region was segmented into ten squares in each direction, each square comprising $40 \times 40 = 1{,}600$ lattice locations, for a grand total of $40 \times 40 \times 10 \times 10 = 160{,}000$ lattice cells. Consequently, the edge of a single cell was 12.5 m. For the purposes of these plots, the common parameter values were as follows: a constant wind speed of 43 km/h, and a wind direction of 45 degrees (meaning in a northeasterly direction). The fine fuel moisture code (FFMC), reflecting the moisture in the top strata of ground-level fuel was 90.9, a very high rating; ground fire would tend to spread quickly under this condition.

Wherever possible, we took our parameter values from the documentation on the Prometheus site (Prometheus 2006). The rates of spread were taken to be constant with respect to terrain and fuel type. Greater variability would be observed from replication to replication if the rates would be allowed to vary with these quantities. We leave such a consideration for future work.

3.1 Calculating the infinitesimal rates

This subsection details the steps in determining the exponential rates for the model. In the Canadian Forest Fire Behavior Prediction (CFFBP) System, the rate of spread (ROS) is calculated as a function of Initial Spread Index (ISI) and fuel type. The ISI, in turn, is a function of windspeed and FFMC.

The first step in calculating ROS involves determining two ISI values: an ISI at 0 wind speed and an ISI at the measured wind speed for the period of interest, that is the ISI evaluated at the pair (wind speed = 0, FFMC), and the ISI evaluated at the pair (period wind speed, FFMC) as determined by a table lookup (Hirsch 1996, Table 6, page 29).

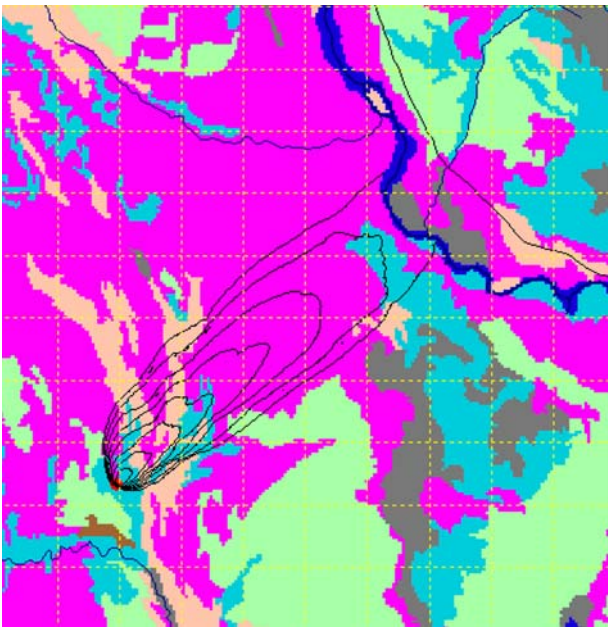

Fig. 2 Prometheus simulation of the Dogrib fire from a point source ignition with Red Deer River set as a fuel break: elapsed time 160 min, Fire size 307.86 ha

For a measured daily wind speed = 43 km/h and FFMC = 91 (Hirsch 1996, Table 6, page 29) gives ISI = 43.0, and for wind speed 0, and FFMC = 91, the same table gives ISI = 5.0. ISI increases quickly with both wind speed and FFMC; therefore, if the wind speed had changed significantly within the time period of interest, repeated ISI measurements would have been needed to handle each period.

The base and maximum ROS use the wind speed = 0 and wind speed = period wind speed ISI values, via either a tabular lookup or reading from a graph (Hirsch 1996). The base ROS and maximum ROS correspond to λ^b and λ^m respectively in Sect. 2.2. These were constant for the period of interest, not depending on time. These values were used in the rate function (9). We also took $c(t) = 1$ in (9); diurnal effects were neglected in the runs presented here.

The ROS value functions are fuel-type-dependent, and are given separately for different fuel types in Hirsch (1996). For Boreal Spruce fuel type (Hirsch 1996, Fig. 12, page 43), with base ISI = 5.0, the base ROS $\lambda^b = 3.0$ m/min, and the maximum ROS $\lambda^m = 66.5$ m/min when ISI = 43. If the fuel type is matted grass, then from (Hirsch 1996, Fig. 23, page 60) one obtains base ROS $\lambda^b = 1.5$ m/min and maximum ROS $\lambda^m = 8.5$ m/min.

The fuel type for this example is mixed, so we used the Boreal spruce ROS values scaled by a multiplicative factor of 0.372. This gave reasonable pictures, but the determination of a rate of spread for mixed fuel types is a subject for further research.

In order to assess a rate of burnout, one needs to consider the depth of the fire front, the rate of spread, together with the duration of typical intense flaming in a particular

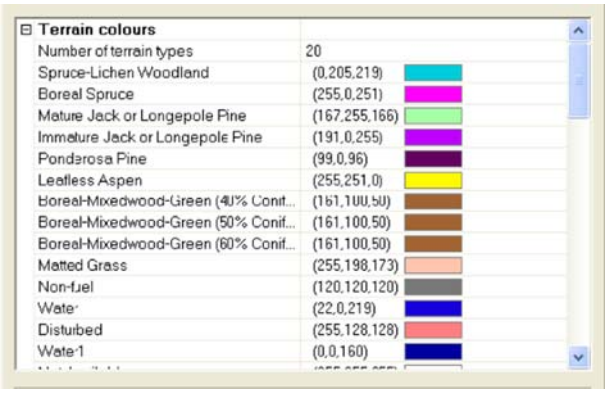

Fig. 3 Legend for the Terrain colour scheme of the Dogrib maps

piece of fuel, which tends to range between 20 and 40 s (see Taylor et al. 2004). For the purposes of the simulation examples presented here, we have assumed that the burnout rate was 0.167 times the maximum ROS at that cell.

The last step is to transform the various rates of spread (distance per unit time) into our various exponential rates as per (9). This was achieved via a linear translation based on the size of the cell (in the Dogrib case, 12.5 m). The exponential rates were then summed as described in (11) to obtain the rates of a lattice cell making the transition from state F to state B.

3.2 Parameter values for the spotting mechanism

Parameter values were chosen on rough physical grounds, but were not based on hard data. Nonetheless, seemingly credible realizations were obtained. The firebrand rate of emissions was 0.016 per minute per cell, roughly 1 per hour per cell. The time a firebrand was aloft was exponentially distributed with a mean of 10 s, and the mean amount of time a firebrand was alight was 100 min, meaning that virtually all firebrands were still burning upon landing. Combining our wind speed and mean time aloft, the mean spotting distance (distance traveled by a firebrand) was 119.4 m. The probability that a live firebrand led to ignition upon landing was 0.7. The variation in the landing location was normally distributed with a standard deviation of 1 cell width (i.e. $\sigma = 12.5$ m) in both axis directions.

3.3 Discussion of the results

The sequence of images presented in Figs. 4, 5 and 6 show the evolution of a single realization after 1, 2, and 3 h of simulated elapsed time. The legend for the colour scheme used is given in Fig. 3 in the Appendix.

Figures 7, 8, and 9 show three sample paths, based on identical parameter values, corresponding to an elapsed time of 160 min. They illustrate the degree of variability

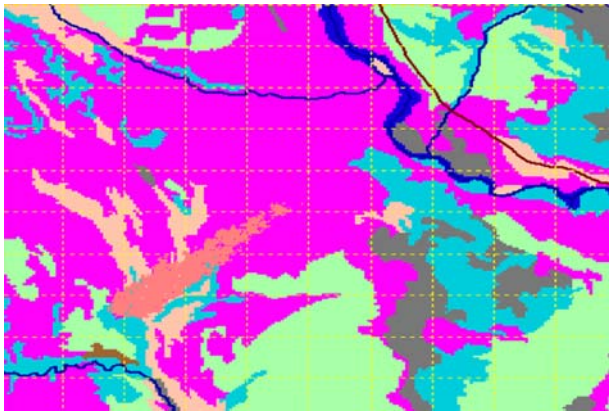

Fig. 4 Simulation of the Dogrib fire: elapsed time 1 h, Fire size 47.52 ha

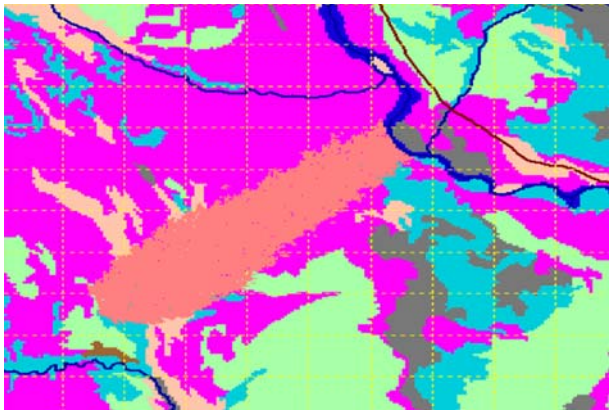

Fig. 5 Continuation of simulation in Fig. 4 of the Dogrib fire: elapsed time 2 h, Fire size 231.12 ha

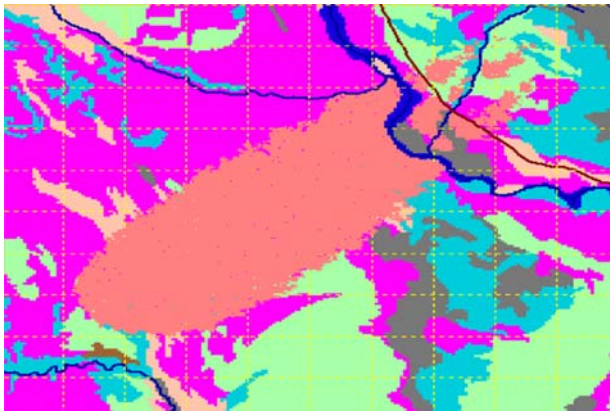

Fig. 6 Continuation of simulation in Fig. 5 of the Dogrib fire: elapsed time 3 h, Fire size 481.66 ha

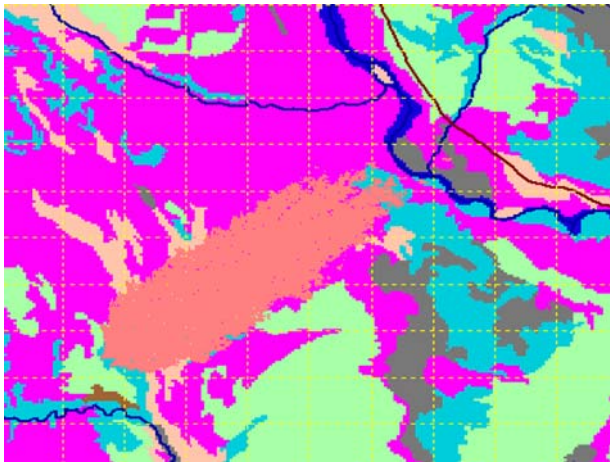

Fig. 7 Replication number 1 of the Dogrib fire: elapsed time 160 min, FJR = 146.39, Fire size 233.64 ha

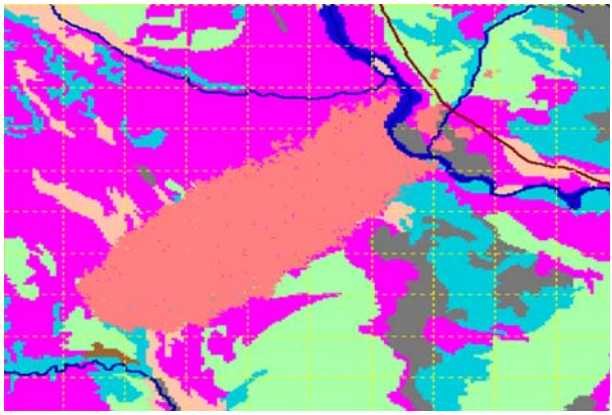

Fig. 8 Replication number 2 of the Dogrib fire: elapsed time 160 min, FJR = 104.7 min, Fire size 377.77 ha

for this stochastic model. The shapes of these fires are similar, being roughly elliptical. The model is sufficiently complex that we are unable to prove that this kind shape will always result (under constant wind direction). One related result has been obtained by Richardson (1973), where a simpler evolving isotropic nearest neighbour lattice model produces a circular shape in the long run, with probability 1.

Because of our fire spotting mechanism, all 600 of our simulated fires succeeded in jumping the Red Deer River, replicating the behaviour of the fire event of October 16. (These 600 runs were conducted in an initial set of 300 runs and a later second set to collect additional information.)

Generally the earlier the spotting fire jumps the river (FJR), the larger the fire across the river. We observe that while the fire depicted in Fig. 7 has crossed the river by time 160 min, there is no meaningful growth yet on its far side. In contrast, from Fig. 8 we

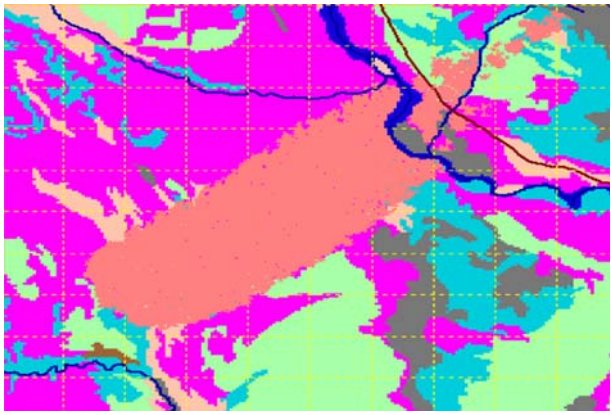

Fig. 9 Replication number 3 of the Dogrib fire: elapsed time 160 min, FJR = 98.1 min, Fire size 420.2 ha

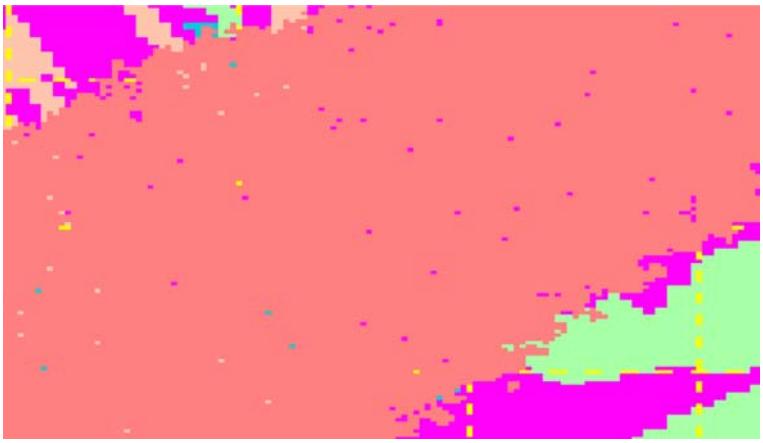

Fig. 10 An enlarged realization revealing unburnt areas

see that this replication has crossed the river, and there is a moderate degree of lateral fire spread on the far side. Figure 9 shows a realization with substantial fire growth that is the direct result of an early river crossing time.

Figure 10 provides an enlargement of a sample run, which reveals small islands of unburnt terrain. Some of these will become burnt as time evolves, and some will remain unburnt when all their nearest neighbours or adjacent cells eventually burn out. If the burn-out rate were to increase relative to the rate of spread, these islands of unconsumed fuel would be larger and more numerous.

We carried out further empirical analyses of the 600 simulation realizations in order to relate the FJR time to the size of the fire after 160 min. This time has a significant impact on the subsequent fire shape and extent of spread. The smallest FJR time was 73.9 while the largest FJR time was 146.39 min. The mean and standard deviation of the FJR times for all 600 realizations were 108.3 and 12.7 min respectively.

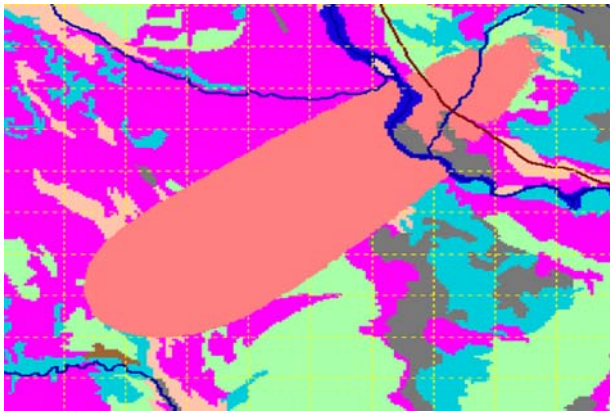

Fig. 11 Dogrib fire: 5% probability contour at elapsed 160 min

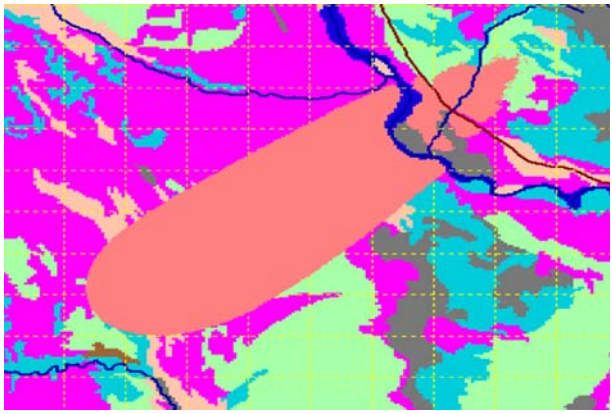

Fig. 12 Dogrib fire: 10% probability contour at elapsed 160 min

There is a negative correlation between FJR time and fire area. We consider the total area burned by 160 min of elapsed time: the smallest fire area was 233.64 ha, while the largest was 473.6 ha, and the mean and standard deviation of the fire area were 382.4 and 29.8 ha respectively. The fire having smallest area had an FJR time of 146.39 min, and the largest fire had an FJR time of 88.7 min. The lowest FJR time of 73.9 min corresponded to a fire having an area of 438.1 ha.

Figures 11, 12, 13 and 14 give simulation estimates of the point wise probability contours of size 5, 10, 50 and 90% respectively, at elapsed time 160 min and based on our initial run of 300 replicates.

The $p\%$ contour plot is the region of points for which $p\%$ of the simulation replicates were burning or had burned at an elapsed time of 160 min. For instance, the 10% contour plot shows those cells that have been reached by fire in at least 10% of the realizations (i.e. at least 30 of the 300 realizations). It is interesting to note that with the 5 point neighbourhood $\mathcal{N}$ given in (1), the shapes of these regions are roughly elliptical. From the 50% figure, however, we can discern that a frequent phenomenon

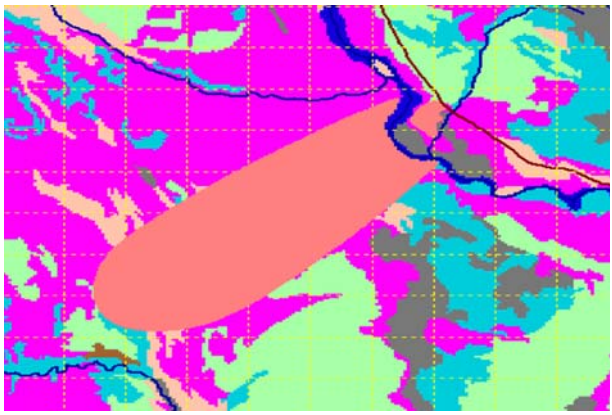

Fig. 13 Dogrib fire: 50% probability contour at elapsed 160 min

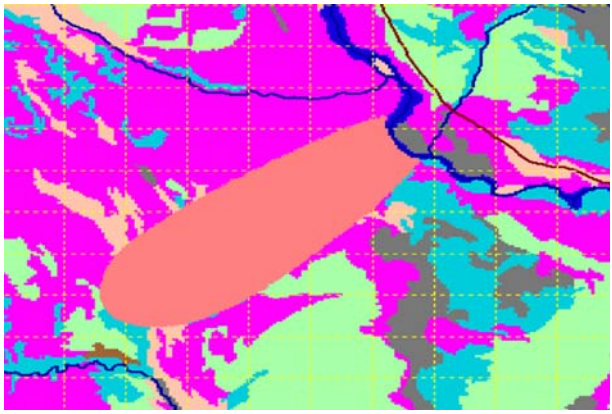

Fig. 14 Dogrib fire: 90% probability contour at elapsed 160 min

is for the fire to spot some distance away from the river, and then to grow upwind as well as downwind. Several deterministic models impose this elliptical shape property (Finney 1999; Richards 1990), whereas it comes naturally from the stochastic structure in this model. Care should be taken in interpreting these plots. For example in Fig. 14, the 90% plot does not cross the river, but this does not mean that 90% of sample paths or realizations do not cross the river. It means that points across the river burn with a point-wise probability of less than 0.9. All the sample realizations crossed the river, but the locations of these spot fires were highly variable.

A referee pointed out that Figs. 11 through 14 all exhibit a similar shape indicating a similarity in burn patterns among all realizations.

The stochastic model, through its simulation output, can also provide other model information, such as the typical fire size by a specified time. Figure 15 shows one such growth curve. Based on our initial set of 300 simulation paths through time, this plot gives the median (50th percentile) fire size at various times. This is similar to the type of information that deterministic models can give, but stochastic models can

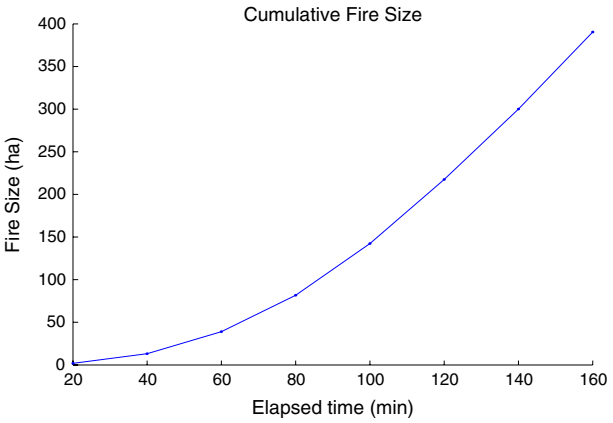

Fig. 15 Cumulative median fire size (ha) for the Dogrib model elapsed time 160 min

also yield plots for other percentiles. For example, plotting the 99th percentile through time provides information about extreme growth.

One might argue that we should start our simulation runs at the same location as the real Dogrib fire, with time $t = 0$ corresponding to the start of the fire on September 25th. However, as has been pointed out by Podur (2006), in attempts to track the impact of large fires, it is much more important to track the major "fire event" successfully, than to track them through stages of minor growth. The Dogrib fire consumed roughly 10 times more in 13 h on October 16th than it had in the previous 21 days. For us to have tracked the Dogrib examples over the entire period of time would have necessitated run times an order of magnitude larger, which would have severely limited our ability to consider as many alternatives as we have.

4 Concluding remarks

In this paper, we have introduced a stochastic fire spread model. At this time, there are several deterministic spread models in use (e.g. Prometheus, Farsite, etc.). We do not intend for the model proposed here to be thought of as a replacement for these existing models. Rather, we intend to provoke discussion and thought about how to enhance or extend such models using a stochastic spread mechanism.

One question that needs to be addressed is whether the exponential distribution assumption is realistic. If the grid cells have small areas, this assumption is likely as reasonable as any, since the aggregate effect over a large number of cells will be essentially independent of the actual distribution for a single cell.

It is essential that a comparison be made of the distribution of simulated fire spread rates with experimental fire spread rates in order to properly validate this model. More comparisons with Prometheus output will also help to test the validity of our proposal.

Acknowledgements The authors express their hearty thanks to Rob MacAlpine of the Ontario Ministry of Natural Resources, Dave Martell of the Faculty of Forestry at the University of Toronto, Mike Wotton of the Canadian Forestry Service and Cordy Tymstra of Alberta Sustainable Resource Development Directorate

for helpful comments on forest fire spread, and more generally on other forestry issues. We also thank the referees, both of whose comments have improved the structure and content of the paper. WJB, RJK, and DAS also wish to thank the Natural Sciences and Engineering Research Council (NSERC), whose funding has supported this work. GEOIDE SII and NPCDS also provided funding support for programming.

References

Anderson KR, Flannigan MD, Reuter G (2005) Using ensemble techniques in fire-growth modelling. In: 6th Symp. on Fire and Forest Meteorology, vol 2.4. Canmore, Alberta Amer Meteorol Soc, Boston, MA, pp 1–6, 24–27, Oct 2005

Berjak SG, Hearne JW (2002) An improved cellular automaton model for simulating fire in a spatially heterogeneous Savanna system. Ecol Model 148:133–151

Boychuk D, Braun WJ, Kulperger RJ, Krougly ZL, Stanford DA (2007) A stochastic model for fire growth. INFOR, Special Issue on Forestry 45:339–352

Forestry Canada Fire Danger Group (1992) Development and structure of the Canadian Forest Fire Behaviour Prediction System. Forestry Canada, Science and Sustainability, Information Report ST-X-3

Chase CH (1984) Spotting distance from wind-driven surface fires—extensions of equations for pocket calculators. Res. Note INT-346. US Department of Agriculture, Forest Service, Ogden UT

Durrett R (1988) Lecture notes on particle systems and percolation. Wadsworth

Finney MA (1999) Mechanistic modelling of landscape fire patterns. In: Mladenoff DJ, Baker WL (eds) Spatial modelling of forest landscape change: approaches and applications, Cambridge University Press, pp 186–209

Hirsch KG (1996) Canadian Forest Fire Behavior Prediction (FBP) System: user's guide. Special Report 7, Canadian Forest Service, Northwest Region, Northern Forestry Centre. UBC Press, Vancouver, BC. ISBN 0-660-16389-6. ISSN 1188–7419

Lewis PAW, Shedler GS (1976) Simulation of nonhomogeneous Poisson processes with log linear rate function. Biometrika 63:501–506

Malamud BD, Morein G, Turcotte DL (1998) Forest fires: an example of self-organized critical behavior. Science 281:1840–1841

Ntaimo L, Zeigler BP, Vasconcelos MJ, Khargharia B (2004) Forest fire spread and suppression in DEVS. Simulation 80(10):479–500

Podur J (2006) Weather, Forest Vegetation, and Fire Suppression Influences on Area Burned by Forest Fires in Ontario. Ph.D. Thesis, Faculty of Forestry, University of Toronto

Prometheus: The Canadian Wildland Fire Growth Model (2006). Web site for current release of Prometheus 4.3.5: http://www.firegrowthmodel.com/index.cfm

Prometheus: The Canadian Wildland Fire Growth Model (2006). Dogrib data and information http://www.firegrowthmodel.com/public_download.cfm

Richards GD (1990) An elliptical growth model of forest fire fronts and its numerical solution. Int J Numer Meth Eng 30:1163–1179

Richardson D (1973) Random growth in a tessleation. Proceedings of the Cambridge Philosophical Society, 74:515–528

Rothermel RC (1972) A mathematical model for predicting fire spread in wildland fuels. USDA For. Serv., Intermt For. and Range Exp. Stn, Ogden, UT. Res. Paper INT-1 15: pp 40

Stauffer D, Aharony A (1992) Introduction to percolation theory. Taylor and Francis, Washington

Taylor SW, Wotton BM, Alexander ME, Dalrymple GN (2004) Variation in wind and crown fire behaviour in a northern jack pine—black spruce forest. Can J Forest Res 34:1561–1576

Trevis L (2005) Master's Thesis. University of Calgary. Electronic version available at http://www.geomatics.ucalgary.ca/Papers/Thesis/NES/05.20222.LTrevis.pdf

Xu J, Lathrop RG (1994) Geographic information system based wildfire spread. In: Proceedings of 12th fire and forest meteorology conference, pp 477–484

Author Biographies

Den Boychuk, BASc, MScF, Ph.D. (Toronto) is an industrial engineer, and has done private consulting applying operational research techniques to problems in forest and forest fire management. He now does

research and operational work in Ontario's forest fire management organization. Current research interests include modelling under risk in areas such as fire growth, contract optimization, short-term planning, and strategic planning.

W. John Braun is Associate Professor of Statistics, University of Western Ontario, receiving his Ph.D. in 1992. His research interests are in stochastic modeling, data analysis and smoothing methods. He applies these in various areas of psychology, mathematical biology, quality control and more recently forestry. He has a recent monograph Data Analysis and Graphics Using R: An Example-based Approach.

Reg J. Kulperger is Professor of Statistics, University of Western Ontario, receiving his Ph.D. in 1978. He has worked on various problems in mathematical statistics and stochastic modeling and statistical inference. The applications are in mathematical biology, finance and time series, and more recently in forest fire models.

Zinovi L. Krougly is an Adjunct Professor/Research Associate in the Departments of Statistical and Actuarial Sciences & Applied Mathematics at the University of Western Ontario. He received his Ph.D. in 1984 from the Institute of Control Problems (Moscow), Russian Academy of Science. He worked at the Central Research Institute for Applied Computer Science in Minsk until 1998. His research interests include performance evaluation and optimization of computer-communication systems, queueing networks, stochastic modelling of natural phenomena, and C++ scientific computing. His previous papers include several in Performance Evaluation, Automation and Remote Control, and elsewhere.

David A. Stanford is a Professor in the Department of Statistical & Actuarial Sciences at the University of Western Ontario. He received his Ph.D. in 1981 from Carleton University, and worked until 1986 at Bell Northern Research in Ottawa. His research interests include queues and risk processes, call centers and telecommunications, and stochastic modelling of natural phenomena. He has published previously in Performance Evaluation, Operations Research, Queueing Systems, Journal of Applied Probability, ASTIN Bulletin, and elsewhere. He is a member and past President of the Canadian Operational Research Society, and a member of INFORMS.